Current Optics and Photonics
Vol. 3, No. 1, February 2019, pp. 16-21

ISSN: 2508-7266(Print) / ISSN: 2508-7274(Online)
DOI: https://doi.org/10.3807/COPP.2019.3.1.016

Comb-spacing-swept Source Using Differential Polarization Delay Line for Interferometric 3-dimensional Imaging

Sang Min Park[1†], So Young Park[2†], and Chang-Seok Kim[1*]

[1]*Department of Cogno-Mechatronics Engineering, Pusan National University, Busan 46241, Korea*
[2]*Component Industry & Automotive Manufacturing Technology Group, Samsung Electro-Mechanics, Busan 46754, Korea*

(Received October 27, 2018 : revised December 5, 2018 : accepted December 6, 2018)

We present a broad-bandwidth comb-spacing-swept source (CSWS) based on a differential polarization delay line (DPDL) for interferometric three-dimensional (3D) imaging. The comb spacing of the CSWS is repeatedly swept by the tunable DPDL in the multiwavelength source to provide depth-scanning optical coherence tomography (OCT). As the polarization differential delay of the DPDL is tuned from 5 to 15 ps, the comb spacing along the wavelength continuously varies from 1.6 to 0.53 nm, respectively. The wavelength range of various semiconductor optical amplifiers and the cavity feedback ratio of the tunable fiber coupler are experimentally selected to obtain optimal conditions for a broader 3-dB bandwidth of the multiwavelength spectrum and thus provide a higher axial resolution of 35 μm in interferometric OCT imaging. The proposed CSWS-OCT has a simple imaging interferometer configuration without reference-path scanning and a simple imaging process without the complex Fourier transform. 3D surface images of a via-hole structure on a printed circuit board and the top surface of a coin were acquired.

Keywords : Comb-spacing-swept source, Differential polarization delay line, Interferometry imaging
OCIS codes : (060.2350) Fiber optics imaging; (110.4500) Optical coherence tomography; (120.3180) Interferometry; (120.4825) Optical time domain reflectometry

I. INTRODUCTION

Various optical interferometry methods have been proposed for three-dimensional (3D) surface profilometry and tomography imaging based on mechanical scanning of the optical path length, including white-light scanning interferometry [1] and coherence scanning microscopy [2]. Spectral interferometry without mechanical scanning has also been proposed to simplify the imaging configuration. This approach uses a wavelength scanning source or detector spectrometer [3, 4]; however, there are practical limitations such as the high cost of a tunable laser source and large number of calculations in the Fourier transform process.

Recently, an alternative light source with frequency-comb generation has been proposed to synthesize the coherence function for the profilometry and tomography [5, 6]. However, this light source has a limited narrow bandwidth of 2 nm, which implies an imaging resolution over 0.3 mm [6].

In this paper, we propose a novel broad-bandwidth multiwavelength light source based on a differential polarization delay line (DPDL) to simultaneously sweep each comb spacing of the multiwavelength spectrum. Various multiwavelength light sources have been suggested mainly for wavelength-division multiplexing (WDM) in optical communication [7] and improved energy efficiency of a spectrally sampled light source [8]. However, no study has been reported on a fast and continuous tuning (sweeping) of the comb spacing of a broad-bandwidth multiwavelength source for interferometry imaging.

†These authors contributed equally to this work.
*Corresponding author: ckim@pusan.ac.kr, ORCID 0000-0002-2811-8137
Color versions of one or more of the figures in this paper are available online.

II. PRINCIPLE

The proposed comb-spacing-swept source (CSWS) employed a DPDL to generate the frequency comb. The DPDL is an optical device which splits the input light within a fiber into two paths with orthogonal polarizations and modulates the relative delay time between the two polarizations [9]. In the Sagnac loop, the light separated by the polarization beam combiner/splitter (PBC) in both clockwise and counterclockwise directions passes through the DPDL. After passing through the DPDL, the recombined light generates a frequency comb owing to the polarization differential delay. The comb spacing of the CSWS is determined by the delay time of the DPDL. Based on a theoretical calculation, the comb spacing is expressed by [9]

$$\Delta\lambda_C = \frac{\lambda_0^{\,2}}{c \cdot \Delta t} \tag{1}$$

where $\Delta\lambda_C$ is the comb spacing along the wavelength, λ_0 is the center wavelength, c is the speed of light in air, and Δt is the delay time of the DPDL in the comb spacing sweeper. According to Eq. (1), the free spectral range (FSR) of the CSWS is inversely proportional to Δt. This implies that we can change the comb spacing of the output spectrum by adjusting Δt.

Based on the theoretical relation in Ref. 6, the optical path difference between the reference and sample arms, nL, of the optical interferometer can be measured by sweeping the comb spacing of the CSWS. The interferometer signal shows a peak interferogram when the following condition is satisfied [6]:

$$nL = \frac{N \cdot \lambda_0^{\,2}}{2 \cdot \Delta\lambda_C} \tag{2}$$

where n is the refractive index of the medium and N is an integer. This implies that the interferogram peaks can be repeatedly monitored by increasing the wavelength comb spacing $\Delta\lambda_C$ over the orders of N. By sweeping the comb spacing between the adjacent orders of N, we can obtain the multiple intensity peaks corresponding to the multiple surface reflections of the sample. Therefore, instead of the reference-path scanning in the conventional time-domain optical coherence tomography (TD-OCT) system, the CSWS tunes the light source spectrum to obtain the time-dependent interferogram of the TD-OCT configuration.

The length resolution ΔL of the optical path difference between the reference and sample arms can be expressed as [6]

$$\Delta L = \frac{\alpha \cdot \lambda_0^{\,2}}{2n \cdot \Delta\lambda_B} \tag{3}$$

where α is a coefficient approximately equal to 1, determined by the envelope shape of the multiwavelength spectrum. This relation shows that the length resolution ΔL is inversely proportional to the 3-dB bandwidth of the light source $\Delta\lambda_B$. The length resolution corresponds to the axial resolution in the interferometric image of the OCT system. The broader bandwidth helps us obtain a higher resolution to clearly distinguish the multiple reflection layers.

III. EXPERIMENTAL SETUP

Figure 1 shows a schematic diagram of the proposed interferometry imaging setup. The system consists of three parts: light source, Michelson interferometer, and electrical control part. The proposed Michelson interferometer is similar to a conventional swept-source optical coherence tomography (SS-OCT) system as it employs neither a free-space spectrometer of spectral-domain (SD) OCT nor a reference-path scanner of TD-OCT [10]. However, instead of the conventional single-wavelength SS, the CSWS is proposed to induce an optical interferogram and obtain depth scanning for tomography imaging. The proposed signal processing method for depth scanning is similar to that of the conventional TD-OCT; however, the periodic scanning of the reference path is replaced by the periodic sweeping of the comb spacing from the inside of the light source.

In the all-fiber CSWS, the light from a semiconductor optical amplifier (SOA) is separated along two polarization states by a PBC and a circulator. A periodic comb-spacing spectrum filter can be implemented using a fiber-pigtailed DPDL (DDL-650-11, Oz Optics). By varying the delay time of the DPDL using an applied external voltage signal, we can sweep the comb spacing for the A-scanning of a depth image. The maximum delay range of the DPDL is ±50 ps, while the delay resolution is 0.0027 ps. The delay time of 50 ps corresponds to a delay length of ~15 mm in the air medium. For the displacement tuning of the DPDL, the

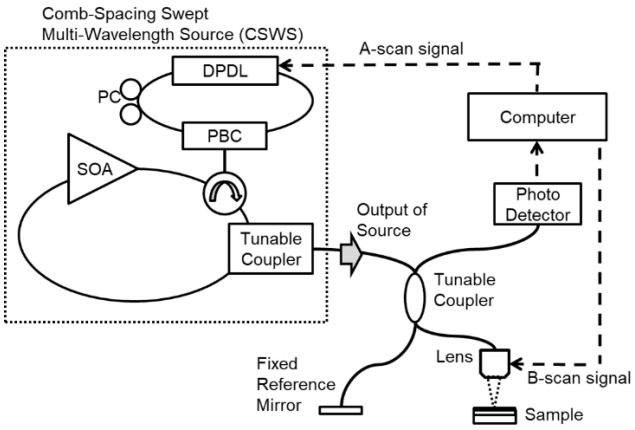

FIG. 1. Experimental setup of the all-fiber interferometer using the multiwavelength CSWS.

speed is 3 ps/s, while the repeatability is smaller than 0.05 ps, which could be easily enhanced if the electrooptic modulation can be applied in the tuning of the DPDL [11]. For a comb-spacing sweeper based on the polarization diversity loop configuration (PDLC), the PBC and circulator can be replaced by a simple 50:50 directional coupler, which is typically used in a fiber Sagnac loop. For the output port, a tunable coupler can be located in the fiber ring cavity to control the cavity feedback ratio from the lasing output.

In the interferometer, the other tunable coupler splits the interfered light into reference and sample paths and combines the reflected light from both paths. The reference path is fixed as there is no need to induce a path-length difference in the Michelson interferometer although the signal processing is the same as that in TD-OCT. A simple B-scanning is used to move the sample path in the lateral direction. An objective lens (LSM02, Thorlabs) with a pupil diameter of 4 mm and focal length of 18 mm was used to obtain an interferometric image in the OCT system. As the numerical aperture (NA) of this objective lens is 0.11, the diameter of the beam focused by the objective lens of the OCT system at 1550 nm is ~18 μm [12]. Therefore, the theoretically estimated lateral resolution of this OCT system at 1550 nm is ~9 μm, which is half of the beam diameter owing to the Rayleigh limit [13, 14].

IV. RESULTS

The comb-spacing variation was experimentally measured while the delay time of the DPDL was linearly changed. As presented in Fig. 2, which shows the output spectra of the CSWS according to the delay time of the DPDL, the comb spacing can be decreased by increasing the delay

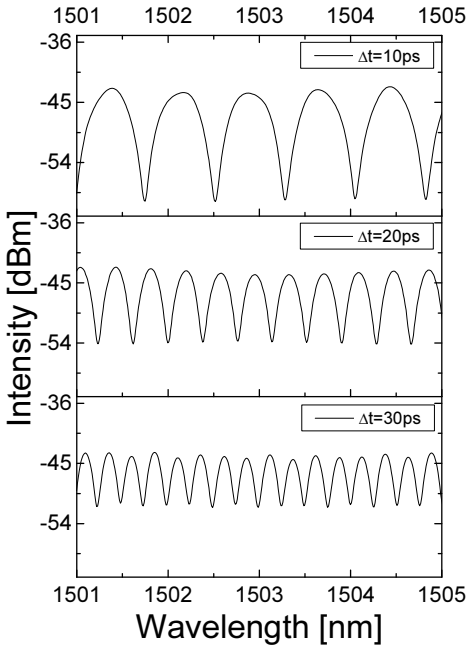

FIG. 2. Multiwavelength source output spectra according to the delay time of the DPDL.

time of the DPDL, Δt. For $\Delta t = 10$, 20, and 30 ps, the measured comb spacings, $\Delta\lambda_C$, were 0.82, 0.40, and 0.27 nm, respectively, which are in good agreement with the values calculated using Eq. (1).

Figure 3 shows the output spectra of the CSWS when the delay time of the DPDL is varied by the A-scanning signal. As shown in Fig. 3(a), when the center wavelength is 1550 nm, the measured $\Delta\lambda_C$ values for $\Delta t = 5$ and 15 ps are 1.6 and 0.53 nm, respectively. Similarly, in Fig. 3(b), when the center wavelength is 1300 nm, the measured $\Delta\lambda_C$ values for $\Delta t = 1.5$ and 15 ps are 3.8 and 0.38 nm,

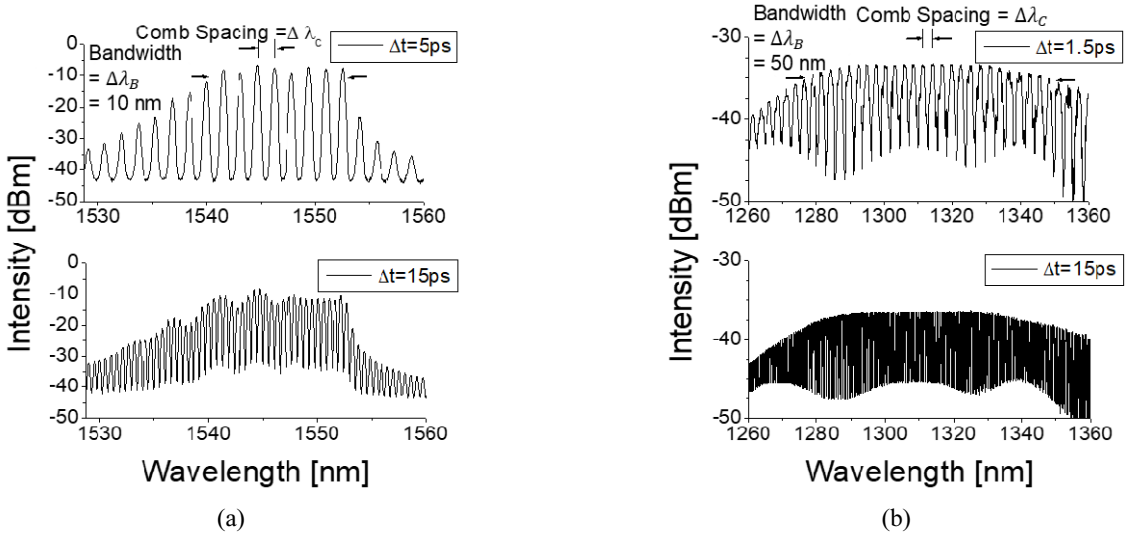

(a) (b)

FIG. 3. Multiwavelength source output spectra with various comb spacings obtained by tuning the delay time, Δt, for output coupler cavity feedback ratios of (a) 70% and (b) 0%.

respectively. For comparison, we employed various experimental setups using a variable-ratio output coupler and various SOAs with center wavelengths of 1550 and 1300 nm. For example, with the increase in the cavity feedback ratio of the output light into the input of the SOA, the output port of the CSWS shows lasing spectra with a larger finesse (ratio of the FSR to the linewidth).

The change in the output spectral bandwidth of the CSWS was measured when the cavity feedback ratio of the output light was tuned. As shown in Fig. 3(a), the output spectrum of the CSWS showed a typical multiwavelength lasing characteristic when we increased the cavity feedback with a cavity feedback ratio of 70%. Owing to the lasing characteristics, the peak intensity increased up to approximately -10 dBm and the finesse increased to approximately 20, as obtained from the optical spectrum analyzer (OSA). However, the 3-dB bandwidth, $\Delta\lambda_B$, of the multiwavelength spectrum became narrower (approximately 10 nm). In contrast, when the cavity feedback ratio of the output coupler was reduced to 0% in Fig. 3(b), the finesse of the multiwavelength spectrum decreased to 2. This corresponds to a simple cascade configuration of the amplified spontaneous emission (ASE) source and sinusoidal comb-spacing spectral filter. For this ASE-type output of the CSWS, the peak intensity is not so high below -35 dBm, obtained from the OSA. However, the 3-dB bandwidth of the multiwavelength spectrum can be significantly broadened over 50 nm, which is equal to the original ASE bandwidth of the SOA.

Therefore, the 3-dB bandwidth of the CSWS could be changed from 10 to 50 nm as the feedback ratio of the output coupler was tuned, from 70 to 0%, respectively. As shown in Eq. (3), the 3-dB bandwidth affects the axial resolution of the interferometric imaging. This implies that the ASE spectrum in Fig. 3(b) will be more useful for a higher-resolution tomography image, compared to the lasing spectrum in Fig. 3(a). For a high axial resolution, the interferometric image was obtained using the broad-bandwidth CSWS output light with a feedback ratio of 0%.

Figure 4 shows the point spread function (PSF) of the proposed interferometer imaging system with the CSWS. For example, as we control the delay time of the DPDL in the CSWS, from 20 to 30 ps, the output spectrum of the CSWS varies its comb spacing, from 0.40 to 0.27 nm, respectively. The periodic sweeping of the comb spacing, from 0.40 to 0.27 nm, corresponds to the A-scanning of the path-length difference of the TD-OCT up to 3.5 mm, repeatedly.

In order to measure the PSF of this OCT system, we installed a mirror on the sample path and detected the fringe burst pattern between the reference and sample lights with a photodetector. A 50/50 fiber coupler was used to divide the CSWS output light into reference and sample paths with equal intensities. By moving the target mirror at intervals of 0.3 mm in the sample path, we could successfully measure a clear PSF up to 3.5 mm in depth; the measured signal-to-noise ratio was approximately 30 dB up to 3.5 mm. As shown in Fig. 4, the amplitude fall-off is smaller than 1 dB at the path length difference of 3.5 mm. The fall-off along a deeper imaging is one of the serious problems of SS-OCT and SD-OCT owing to the effects of limited spectral resolution and sampling upon the spectral interferogram [10]. However, this problem is not monitored in the proposed OCT system as we use the simple signal processing of the TD-OCT without Fourier transform. It is expected that the intensity of the interferogram is not affected by the relative distance between the reference and sample paths when the generation of the interference signal is induced from the CSWS in the proposed OCT system [6]. According to Eq. (3), the theoretical axial resolution is 24 μm when the center wavelength is 1550 nm, while the spectral bandwidth is 50 nm. The 6-dB bandwidth of the PSF up to 3.5 mm was measured in the range of 24 to 35 μm. The average value of the measured axial resolution is 28 μm, which corresponds to the theoretically expected axial resolution of 24 μm. This degradation of axial resolution seems to originate from the insufficient sampling rate in the measurement of the PSF.

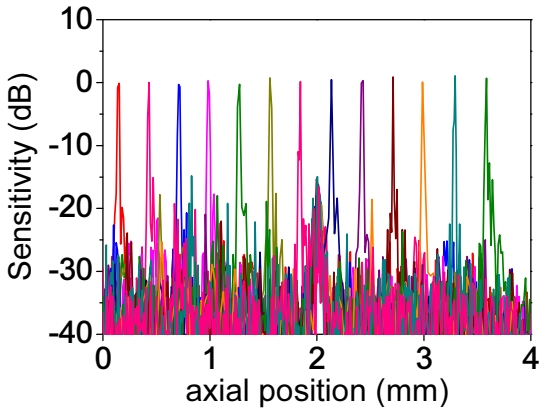

FIG. 4. PSF of the proposed interferometry imaging system.

For the multiple-layered tomography imaging experiment, we prepared samples using a cover glass with a thickness of 170 μm, which were analyzed with the CSWS using an SOA of the 1550-nm region. A printed circuit board (PCB) and Korean 10-won coin were also prepared for the top-surface profilometry experiment. Figures 5(a) and 5(b) show axial A-scan interferogram signals obtained from one and three sheets of the cover-glass sample, respectively. We swept the comb spacing, from 1.6 to 0.53 nm, which correspond to delay times of 5 to 15 ps, respectively.

By gathering the B-scanning data along the lateral positions, we acquired two-dimensional (2D) tomography images, shown in Figs. 5(c) and 5(d), which correspond to the A-scan interferogram signals in Figs. 5(a) and 5(b), respectively. The depth range of tomography can be simply extended by increasing the delay time of the DPDL and decreasing the NA of the objective lens.

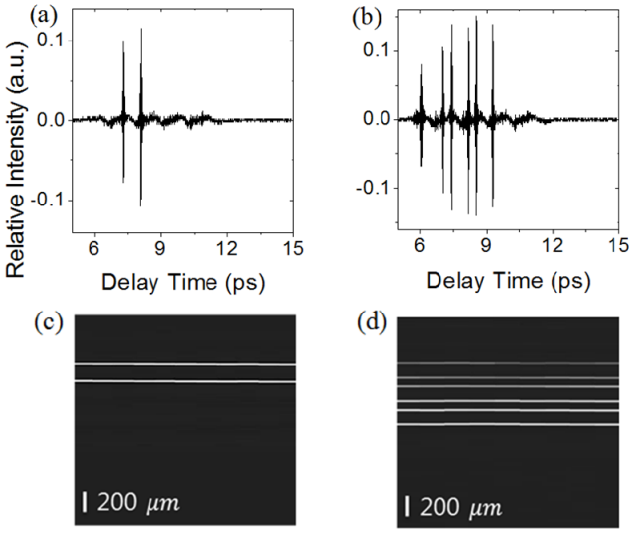

FIG. 5. One-dimensional interferometer signals from (a) one and (b) three sheets of the glass sample. 2D tomography images from (c) one and (d) three sheets of the glass sample.

We also acquired top-surface profile images of via holes on the PCB using the 1550-nm SOA and Korean 10-won coin with the CSWS using the SOA of the 1300-nm region. The via hole is a cylindrical hole structure of epoxy polymer between two copper clad layers. The depth of the via hole is 104 μm, while its diameter is 110 μm. Figure 6(a) shows an optical microscopy image of the via holes on the copper clad laminate (CCL). The result of the profile measurement is shown in Fig. 6(b). The CCL was measured by moving it in the lateral direction for a lateral size of 1.4 μm per pixel (Fig. 6(b)). According to the edge response on the boundary of the via hole, the measured lateral resolution was approximately 10 μm, similar to the theoretically expected value. The 3D surface profile of the coin is also successfully demonstrated in Fig. 6(d) by sweeping the comb spacing of the CSWS for an axial position and scanning the objective lens for lateral positions.

V. CONCLUSION

In this study, the sweeping of the comb spacing of the broad-bandwidth multiwavelength source was experimentally implemented by a tunable DPDL to obtain depth scanning for both top-surface profilometry and multilayer tomography. The signal processing of the proposed CSWS OCT was significantly simpler than that of the single-wavelength SS interferometry in the conventional SS-OCT. The interferometer structure of the all-fiber source scanning type was simpler than those of the conventional interferometer setups using the free-space spectrometer and reference-path scanner in the conventional SD- and TD-OCTs, respectively.

ACKNOWLEDGEMENT

This work was supported by a 2-year Research Grant of Pusan National University.

REFERENCES

1. L. Deck and P. de Groot, "High-speed noncontact profiler based on scanning white-light interferometry," Appl. Opt. **33**, 7334-7338 (1994).
2. B. Lee and T. Strand, "Profilometry with a coherence scanning microscope," Appl. Opt. **29**, 3784-3788 (1990).

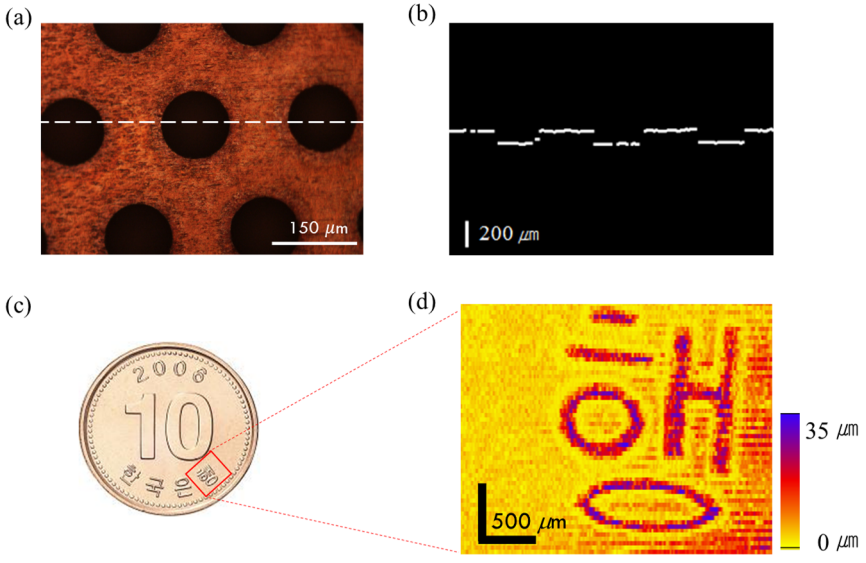

FIG. 6. (a) Via-hole image obtained using an optical microscope and (b) 2D profile image obtained using the CSWS. (c) Coin image obtained using an optical microscope and (d) 3D profile image obtained using the CSWS.

3. L. L. Deck, "Fourier-transform phase-shifting interferometry," Appl. Opt. **42**, 2354-2365 (2003).
4. Y. S. Ghim and S. W. Kim, "Spectrally resolved white-light interferometry for 3D inspection of a thin-film layer structure," Appl. Opt. **48**, 799-803 (2009).
5. Z. He and K. Hotate, "Synthesized optical coherence tomography for imaging of scattering objects by use of a stepwise frequency-modulated tunable laser diode," Opt. Lett. **24**, 1502-1504 (1999).
6. S. Choi, M. Yamamoto, D. Moteki, T. Shioda, Y. Tanaka, and T. Kurokawa, "Frequency-comb-based interferometer for profilometry and tomography," Opt. Lett. **31**, 1976-1978 (2006).
7. C. S. Kim, R. M. Sova, and J. U. Kang, "Tunable multi-wavelength all-fiber Raman source using fiber Sagnac loop filter," Opt. Commun. **218**, 291-295 (2003).
8. E. J. Jeong, J. S. Park, M. Y. Jeong, C. S. Kim, T. J. Eom, B.-A. Yu, S. Gee, J. Lee, and M. K. Kim, "Spectrally-sampled OCT for sensitivity improvement from limited optical power," Opt. Express **16**, 17457-17467 (2008).
9. S. Chung and B. Lee, "Variable wavelength-spacing tunable filter using polarization differential delay line," Opt. Eng. **44**, 020501 (2005).
10. R. Leitgeb, C. K. Hitzenberger, and A. F. Fercher, "Performance of Fourier domain vs. time domain optical coherence tomography," Opt. Express **11**, 889-894 (2003).
11. S. J. Lee, B. Widiyatmoto, M. Kourogi, and M. Ohtsu, "Ultrahigh scanning speed optical coherence tomography using optical frequency comb generators," Jpn. J. Appl. Phys. **40**, L878 (2001).
12. N. V. Iftimia, G. Peterson, E. W. Chang, G. N. Maguluri, W. J. Fox, and M. Rajadhyaksha, "Combined reflectance confocal microscopy-optical coherence tomography for delineation of basal cell carcinoma margins: an *ex vivo* study," J. Biomed. Opt. **21**, 016006 (2016).
13. B. Wang, R. Lu, Q. Zhang, and X. Yao, "Breaking diffraction limit of lateral resolution in optical coherence tomography," Quant. Imaging Med. Surg. **5**, 243-247 (2013).
14. Z. Tong and O. Korotkova, "Beyond the classical Rayleigh limit with twisted light," Opt. Lett. **37**, 2595-2597 (2012).